REVIEW PAPER

Impact Analysis of Concrete Structural Components

A. Rama Chandra Murthy[*], G.S. Palani, and Nagesh R. Iyer

Structural Engineering Research Centre, CSIR, Chennai
[*]*E-mail: murthyarc@sercm.org, archandum@yahoo.com*

ABSTRACT

This paper presents an overview on the concrete structural components subjected to impact loading. The review includes empirical formulae, analytical models, and numerical simulations. Various empirical formulae on penetration depth, perforation, and scabbing limits as well as their ranges of application have been provided. It has been observed that the information available on the validation of these models is limited. There is wider scope to study the performance of well known empirical formulae. Penetration resistance function play an important role in any analytical model. It has been observed that the major limitation is rigid projectile assumption. There is scope to develop new/improved analytical models to represent projectile characteristics. The numerical simulation of concrete structural components subjected to impact loads is a complex phenomenon. From the review, it is observed that employing appropriate material model for concrete, equation-of-state, contact algorithm and definition of yield surface plays significant role in the accurate simulation of concrete structural components. There is ample scope to develop improved methodologies in terms of development of material models and contact algorithms, which can be employed in nonlinear explicit finite element analysis of concrete structural components subjected to impact loading.

Keywords: Concrete structures, reinforced concrete, concrete material models, finite element analysis, impact loading, numerical simulations, impact analysis, compact behaviour

1. INTRODUCTION

Concrete has been widely used over many years by military and civil engineers in the design and construction of protective structures to resist impact and explosive loads. Potential missiles/projectiles include kinetic munitions, vehicle and aircraft crashes, fragments generated by military and terrorist bombing, fragments generated by accidental explosions and other events (e.g., failure of a pressurised vessel, failure of a turbine blade or other high-speed rotating machines), flying objects due to natural forces (tornados, volcanos, meteoroids), etc. These projectiles vary broadly in their shapes and sizes, impact velocities, hardness, rigidities, impact attitude (i.e., obliquity, yaw, tumbling, etc.) and produce a wide spectrum of damage to the target. Impacting missiles can be classified as either hard or soft depending upon whether the missile deformability is small or large relative to the target deformability. Hard projectile impact results in both local wall damage and in overall dynamic response of the target wall. Local damage consists of spalling of concrete from the front (impacted) face and scabbing of concrete from the rear face of the target together with missile penetration into the target. Overall dynamic response of the target wall consists of flexural deformations. A potential flexural or shear failure will occur if the local strain energy capacity of the wall does not exceed the kinetic energy input to the wall by the striking hard missile.

The effects of the impact of a hard projectile on a concrete target have been studied since mid-1700s mainly due to the continuous interest in designing high-performance missiles and protective barriers. The recent requirement to assess the safety of concrete containment vessels for nuclear reactors has also contributed considerably to the current understanding of local impact effects on concrete targets. The initial stiffness of target as well as the ultimate strength increases both in compression and tension. Further, the concrete-strain capacity increases under dynamic loading due to tension stiffening. When a projectile of certain mass and velocity hits a concrete target, concrete generally crushed and cracked, and the structure experiences shaking and vibration depending on the relative period of structure and impact pulse duration. The pressure at the front of the nose of the projectile is several times higher than the static uniaxial strength and lateral confining pressure of concrete. In addition, stress waves may propagate from the tip of the nose of the projectile. Since concrete is very weak in tension, the tensile wave generated when the compressive wave hits the backside of the component may cause scabbing at the backside and cracking in lateral direction. Both the compressive strength and tensile strength of concrete are thus important parameters for evaluating the depth of penetration. The crater size depends on the tensile strength. Both small-scale lab tests and full-scale prototype tests have been used to study impact on concrete targets. These have led to various empirical formulae and analytical models to understand the impact behaviour. The depth of penetration is a function of the impact velocity, angle of inclination of impact, mass and

shape of the projectile and target.

There are three important approaches for studying local effects on a concrete target arising from projectile impact, namely experimental, analytical, and numerical methods. Experimental data are always important for extending the understanding of impact phenomena and for validating analytical and numerical models. Empirical formulae based on experimental data are especially important due to the easiness and simplicity to represent the complex phenomena. Several design codes employ empirical formulae for the design of protective barriers. Simple and accurate analytical models can be developed when the underpinning mechanics of the local effects of the missile impact are understood. This approach offers the most efficient and economic way of predicting these effects and helps to extend the range of validity of empirical formulae based on experiments.

With the rapid development of testing procedures, computational tools, computational mechanics, and material constitutive models, the numerical simulation of projectile impact effects becomes more reliable and economical[1-8]. To get a first order approximation of projectile impact effects, empirical formulae can be useful. In the case of an analytical model, representation of projectile as rigid is a major limitation, i.e., the deformation and failure of the projectile are negligible. The deformation and damage of the projectile may become important either when the impact velocity is high or when the hardness of the projectile is low. There is scope to improve the analytical model by changing the projectile characteristics. Many material models are used in finite element simulation. Each material model requires special material parameters/constants to conduct analysis. Further, specific limitations are built-in for each material model.

2. BACKGROUND

Local and overall impact phenomena for hard missile impact are schematically shown in Fig. 1. With very low velocities, the missile will strike the target wall and bounce off without creating any local damage. As the velocity increases, pieces of concrete are spalled (ejected) off the front or impacted face of the target. This spalling forms a spall crater that extends over a substantially bigger area than the cross-sectional area of the striking projectile. As the velocity continues to increase, the projectile will penetrate the target to depths beyond the depth of the spall crater, forming a cylindrical penetration hole with a diameter only slightly bigger than the missile diameter. As the penetration depth increases, the projectile will stick to the concrete target rather than rebounding. At this stage the impact meets the criteria of a plastic impact. However, even at lesser penetration depths, the impact can be approximately treated as a plastic impact when determining the energy absorbed by the impacted target. Further increase in velocity produces cracking of the concrete on the back surface followed by scabbing (ejection) of concrete from this rear surface. The zone of scabbing will generally be much wider but not as deep as the front-face crater. Once scabbing begins, the depth of penetration will increase rapidly. For

low barrier thickness-to-projectile diameter ratio (<5) the pieces of scabbed concrete can be large in size and have substantial velocities. As the projectile velocity increases further, perforation of the target will occur as the penetration hole extends through to the scabbing crater. Still higher velocities will cause the projectile to exit from the rear face of the target. Upon plastic impact, portions of the total kinetic energy of the impacting projectile are converted to strain energy associated with deformability of the projectile and energy losses associated with target penetration. The reminder of the energy is absorbed or given as input to the target. This absorbed energy results in overall target response that includes flexural deformation of the target barrier and deformation of its supporting structure.
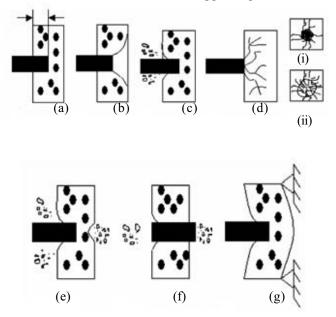

Figure 1. Missile impact effects on concrete target: (a) penetration, (b) cone cracking, (c) spalling, (d) cracks on: (i) proximal face and (ii) distal face, (e) scabbing, (f) perforation, and (g) overall target response.

3. EMPIRICAL FORMULAE

Hanchak[9], *et al.* compared the penetration resistance for concrete specimens with unconfined compressive strengths of 40 MPa and 140 MPa, showing only minor difference in protective performance for projectiles with length/diameter *(L/D)* = 5.66 and caliber radius head (CRH) = 3.0. The predicted penetration depth values using the empirical formulae were lower compared to experimental values in the case of high-trength concrete. David and Yankelevsky[10] analysed the local response of concrete slabs to low-speed missile impact and compared the results with those predicted by the empirical formulae proposed by Petry, the Army Corps of Engineers, NDRC, Kar and UKAEA. But the comparison was done for limited experimental studies and inconsistencies in results were observed. Teland and Sjol[11] predicted penetration depth employing various empirical formulae. It was observed that there had been large variations for predicted penetration depth between different formulae when penetration of flat-nosed projectiles in concrete was

considered. Hakan and Hansson[12] conducted studies using Conwep formula to predict penetration depths of projectile in concrete and the predicted values were compared with the experimental observations. Modifications and limitations for the Conwep formula were suggested to consider projectiles with a length-to-diameter ratio between 6 and 10 and with caliber head radius between 2 and 6. The modified model exhibited a fair agreement with the experimental penetration depth as mentioned in the literature. To the best of authors' knowledge, the information on the performance and applicability of well known empirical formulae is scanty. There is scope and need for studying the performance of these empirical formulae for evaluation of penetration depth in concrete.

Several empirical formulae are available in the literature for evaluation of penetration depth, scabbing limit, and perforation limit. The details of important empirical formulae are given in *Appendix 1* as Table 1.

3.1 Observations

Most of the empirical formulae are obtained by curve fitting test data and are unit-dependent. The empirical formulae are limited by the range of validity, applicable within the limits of the tests from which the data were acquired. Further, it is observed that most of empirical formulae are dimensionally inhomogeneous, which makes it difficult to conduct parametric analysis. From the review, it was observed that the penetration depth values computed by employing Conwep and Haldar formulae exhibit better performance.

4. ANALYTICAL MODELS

Local impact effects of a hard (rigid) projectile on a concrete target are based on the assumption that the deformation and the failure of the projectile are negligible. The deformation and damage of the projectile may become important either when the impact velocity is high or when the hardness of the projectile is low. The concrete target is idealised as a homogeneous material for simplicity in most analytical models. The overall target response is normally neglected and most models focus on local impact analysis. However, the overall target response might play an important role in local missile impact effects for low impact velocities and/or high structural flexibilities. Several analytical models are available in the literature[42-46].

4.1 Formulation of the Penetration Resistance of Target

The critical issue in an analytical penetration model is to formulate the resultant penetration resistance force, FR, applied on the projectile by the target medium during the penetration process. The linear motion of the rigid projectile is governed by Newton's second law:

$$M \frac{dV}{dt} = -F_R \qquad (1)$$

with initial conditions

$$V = V_0 \quad \text{at} \quad t = 0 \text{ and } X = 0 \text{ at } t = 0 \qquad (2)$$

where, $V = dX/dt$, X and V are the instantaneous penetration depth and projectile velocity, M is the mass of the projectile Equations (1) and (2) control the motion of the projectile and thus, the penetration depth.

The penetration resistance has been formulated as a function of the projectile velocity to include the dynamic effects in a penetration process[47]. Often, the penetration resistance takes the form of a binomial function of the instantaneous projectile velocity[48,49] as

$$F_R = F_R(V) = A_1 + A_2 + A_3 V^2 \qquad (3)$$

where, A_1, A_2, and A_3 can be treated approximately as constant parameters determined by the geometry of the projectile nose and the mechanical properties of the target. It has been shown by Forrestal[50], *et al.* that a two-term penetration resistance (i.e., $A_2 = 0$ in Eqn. (3)) gave excellent agreement with instrumented experimental results, which, however, under-estimated the experimental results for a 39 MPa concrete target when the CRH of the projectile becomes large. A more realistic expression of the resistance function[34] is:

$$F_R = A(a + bV^2) \qquad (4)$$

where, A is the cross-sectional area of the projectile nose ($A = A_0$ when the projectile nose is completely embedded into the target, where A_0 is the cross-sectional area of the projectile shank) and a and b are constants to be determined by the geometry of the projectile nose and the mechanical properties of the target.

A linear expression for the penetration resistance was suggested by We[51,52] as

$$F_R = A\left(\alpha f_c + \beta \sqrt{\rho f_c}\, V\right) \qquad (5)$$

where, f_c is a measure of the quasi-static target material strength and α and β are constants that are determined either theoretically or experimentally. Values of α, β and f_c were recommended for four common nose shapes and various target materials and reasonable agreement between predictions and experimental data were obtained for a collection of penetration and perforation tests.

In the last decade, the dynamic cavity expansion theory has been applied to study deep penetrations for metal, concrete, and soil targets[54-56]. Li and Chen[53] further extended Forrestal's concrete and penetration model[55,57] to projectiles of general nose shapes and two independent non-dimensional parameters were introduced to determine the penetration depth. When the interface friction between the projectile nose and concrete medium is neglected, the axial resistance force on the projectile nose can be expressed as[53,57]:

$$F_R = cx \quad \text{for} \quad x < kd \qquad (6)$$

during cratering (related to spalling) and tunneling, where

$$F_R = \frac{\pi d^2}{4}(Sf_c + N^* \rho V^2) \quad \text{for} \quad x^3 kd \qquad (7)$$

$$c = \frac{\pi d}{4k} \frac{(N^* \rho V_0^2 + Sf_c)}{(1 + (\pi k d^3 / 4M)N^* \rho)} \qquad (8)$$

where $S=72.0f_c^{-0.5}$ (9)

$$k=\left(0.707+\frac{h}{d}\right) \quad (10)$$

$$N^*=-\frac{8}{d^2}\int_o^h \frac{yy'^3}{1+y'^2}\ dx \quad (11)$$

where, d is diameter of the proectile, v is velocity of the projectile, M is mass of the projectile, p is density, c is constant, and x is the distance from the projectile.

In addition to the projectile velocity, penetration depth has been considered in the formulation of the penetration resistance function, i.e.,

$$F_R=F_R(x;V) \quad (12)$$

A polynomial function of X and V was introduced by Murff and coyle[58] for penetration:

$$F_R=A_1+A_2x+A_3x^2+A_4V+A_5Vx+.... \quad (13)$$

where, coefficient A_i were determined from experimental data for different projectile diameters, nose lengths, and impact velocities.

An approximate penetration theory, based on a separable form was employed to help the establishment of the modified NDRC formula[15,22], viz.,

$$F_R=g\left(\frac{x}{d}\right)f(V) \quad (14)$$

where, the function g, which is non-dimensional, is given by

$$g\left(\frac{x}{d}\right)=\begin{cases} \dfrac{x}{2d} & \text{for } \dfrac{x}{d} \pounds 2.0, \\ 1 & \text{for } \dfrac{x}{d}>2.0 \end{cases} \quad (15)$$

and

$$f(V)=\frac{1466\sqrt{f_c}}{N^*}\left(\frac{V}{12,000d}\right)^{0.2} \text{(Imperial)} \quad (16)$$

or $$f(V)=\frac{121.7\sqrt{f_c}}{N^*}\left(\frac{V}{1000d}\right)^{0.2}\ (SI) \quad (17)$$

where, N^* is the nose shape factor defined in the modified NDRC formula. Equations (14)-(17) together with Eqns (1) and (2) lead to the modified NDRC penetration formula.

Riera[59] suggested an alternative function, the β function, of the normalised penetration distance. The resistance function was independent of V, i.e., in Eqn (14), $f(V)=1$ and

$$g\left(\frac{x}{d}\right)=\frac{\pi d^2 f_c}{4}\beta\left(\frac{x}{d}\right), \quad (18)$$

where $$\beta\left(\frac{x}{d}\right)=\frac{\beta_1-\beta_2\exp(-cx/d)}{N^*}$$

where, N^* is the nose factor introduced in the modified NDRC formula. Based on Equations (1), (2) and (18), the penetration formula was given in terms of the impact factor introduced by Haldar & Hamieh[39] and β_1 β_2 and c were obtained through a regression method by fitting experimental data on penetration depth as given by Haldar & Hamieh[39] to give

$$I_a=194.59\left(\frac{x}{d}\right)-322.27\left[1-exp\left(-0.598\frac{x}{d}\right)\right] \quad (19)$$

where I_a is defined in Haldar-Hamieh formula.

4.2 Observations

Most of the analytical models are based on the assumption that the deformation and failure of the projectile are negligible. The deformation and damage of the projectile may become significant either when the impact velocity is high or when the hardness of the projectile is low. Normal impact is assumed in most of the models. The important aspect in an analytical model is to formulate the resultant penetration resistance force. The target resistance to penetration is to be represented properly. From the review, it is observed that the models proposed by Forrestal and Tzou[49] and Forrestal[50], et al. seem to be reliable.

5. NUMERICAL SIMULATION
5.1 Numerical Simulation for Concrete Targets

Numerical simulations of dynamic structural response have become increasingly important for concrete structural design against impact loads. In contrast to empirical formulae, these provide information on stress and deformation fields, which may be used to improve the resistance of the concrete. There are several commercial codes available for impact simulations, namely, LS-DYNA, AUTODYN, and ABAQUS. Generally, numerical simulations are based on interactions between material elements or particles, coupled with material constitutive models. Various discrete methods have been applied for concrete media to meet the requirements of application to impact loads. These include the finite difference methods (FDM), finite element methods (FEM), boundary element method, mesh-free methods (e.g., smooth particle hydrodynamics (SPH)), etc. The discrete element methods (DEM) capture the damage and failure features of brittle solids. As with FEM, the space of the medium is mapped on to an assembly of indivisible elements. Proper interactions between elements are defined based on the mechanical properties and cohesion of the medium. A fracture (failure) criterion needs to be satisfied at each step for the validity of the interactive laws. Meanwhile, collision laws are used to determine the repulsive interactions for failed elements. Over the last 30 years, many finite element models for reinforced concrete structures have been developed. However, this area still needs further research; mainly because of the difficulty in modelling concrete for FE analysis. Reinforced concrete has a very complex behaviour, involving factors such as:
- nonlinear stress-strain response, including tensile cracking bi-axial stiffening, and strain softening,
- material failure under multiaxial stress state,

- post-fracture behaviour, and
- interaction between the concrete and reinforcement.

Most concrete models employed in numerical simulations are based on phenomenological descriptions of its macroscopic behaviour obtained in unixial and triaxial loadings. Concrete behaviour under compression is most important for impact applications. It has been widely accepted that the unconfined uniaxial compressive stress-strain relation can be divided into three regimes, as shown in Fig. 2.
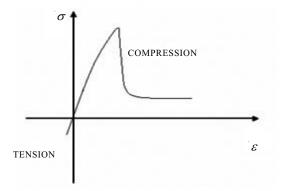

Figure 2. Typical uniaxial compressive stress-strain relation for concrete.

The most frequently used phenomenological concrete model is the combination of an equation-of-state (EOS) in hydrostatic-stress space, an elastic-plastic deformation and failure model (*i.e.*, a strength model) in deviatoric stress space, as an extension of the metal plasticity model (e.g. Meyers,[60]). For an elastic-plastic deformation and failure model, nonlinear plasticity theory with a hydrostatic-dependent yield surface and a non-associated flow rule is generally employed in the nonlinear hardening regime. A failure surface is required to define the initiation of the strain-softening regime in both tension- and compression-dominated stress states. As soon as the failure surface is reached, either the concrete elements are eliminated or a post-failure damage model defined by the residual stress states is applied.

One of the major challenges associated with modelling the behaviour of reinforced concrete is the difficulty of incorporating realistic material models that can accurately represent the physical system. Extensive research over the past two decades has resulted in a variety of constitutive models that are capable of representing the various aspects of concrete behaviour[61-67]. Given the complex behaviour of concrete, large number of distinctly different constitutive models for concrete have been developed. Concrete material formulations can be classified into elasticity-based models, plasticity-based models, plastic-fracturing models, elastic-plastic-damage models, and endochronic models.

5.2 Finite Element Modelling of Reinforced Concrete

The explicit FEM has proven to be an effective tool, especially for transient and impact analyses.

5.2.1 Finite Element Modelling Techniques

The FEM for reinforced concrete structures have generally been based on replacing the composite continuum by an assembly of elements representing the concrete and the steel reinforcement. From the literature, it has been observed that three techniques are mainly employed for modelling reinforcement in a 3-D FEM of a concrete structure: smeared model, embedded model, and discrete model. The specific technique is chosen depending on the application and the degree of detail in which the model needs to be developed. However, most of the difficulties in modelling reinforced concrete behaviour depend on the development of an effective and realistic concrete material formulation and not in the modelling of the reinforcement[68-76].

5.2.1.1 Smeared Model

In the smeared model, the reinforcement is assumed to be uniformly distributed over the concrete elements, (Fig. 3). As a result, the properties of the material model in the element are constructed from individual properties of concrete and reinforcement using composite theory. This technique is generally applied for large structural models, where reinforcement details are not essential to capture the overall response of the structure.
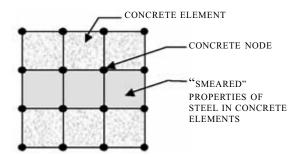

Figure 3. Smeared formulation for reinforced concrete.

5.2.1.2 Embedded Model

To overcome mesh dependency in the discrete model, the embedded formulation allows independent choice of concrete mesh, as shown in (Fig. 4). In this approach, the stiffness of the reinforcement elements is evaluated independently from the concrete elements, but the element is built into the concrete mesh in such a way that its displacements are compatible with those of surrounding concrete elements. The concrete elements and their intersection points with each reinforcement segment are identified and used to establish the nodal locations of the reinforcement elements. The embedded formulation is generally used with higher-order elements. In concrete structures where reinforcement modelling is complex, the embedded representation is advantageous. However, the additional nodes required for the reinforcement increase the number of degrees of freedom (DOFs), and hence the solution time. Further, researchers[77] have found that although analyses with the embedded representation are in general more computationally efficient than those with the discrete representation.
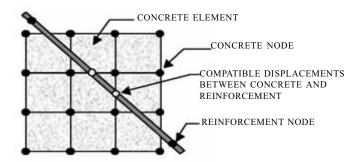
Figure 4. Embedded formulation for reinforced concrete.

5.2.1.3 Discrete Model

In the discrete model, reinforcement is modelled using bar or beam elements connected to the concrete nodes. As a result, there are shared nodes between the concrete element and the reinforcement element, (Fig. 5). Also, since the reinforcement is superimposed in the concrete mesh, concrete exists in the same regions occupied by the reinforcement. The drawback of using the discrete model is that the concrete mesh is restricted by the location of the reinforcement. Full bond is generally assumed between the reinforcement and the concrete. In cases where bond issues are of importance, fictitious spring elements are used to model bond slip between the concrete and the reinforcement elements. These linkage elements connect concrete nodes with reinforcement nodes having the same coordinates. These types of elements have no physical dimension at all and only their mechanical properties are of importance.
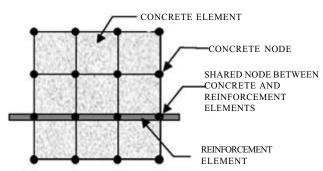

Figure 5. Discrete model of reinforced concrete.

5.3 Contact Algorithms

Several contact algorithms are available in the literature, namely, frictional sliding, single-surface contact, nodes impacting on a surface, tied interfaces, 1-D slide lines, rigid walls, material failure along interfaces, penalty and Lagrangian projection options for constraint enforcement and fully automatic contact[78-81]. Details of a typical algorithm, automatic-single-surface contact are enumerated:

This algorithm uses a penalty method to model the contact interface between the different parts. In this approach, the slave and master surfaces are generated automatically. The method consists of placing normal interface springs to resist interpenetration between element surfaces. An example of this approach is illustrated in Fig. 6. It shows
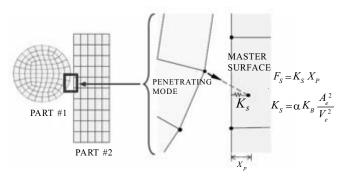

Figure 6. Penalty method for contact algorithm.

that, when a slave node penetrates a master surface in a time step, the algorithm automatically detects it, and applies an internal force to the node (represented by the spring) to resist penetration and keep the node outside the surface. The internal forces added to the slave nodes are a function of the penetrated distance and a calculated stiffness for the master surface. The stiffness is computed as a function of the bulk modulus, volume, and surface area of the elements in the master surface. A static and dynamic coefficient of friction of 0.8 was used between different parts in contact.

5.4 Material Models

There are several material models to represent concrete, which have been implemented in commercial software used for simulation of concrete structures subjected to impact loads. For example, the Drucker-Prager/Cap model and cracking model are available in ABAQUS. LS-DYNA has several concrete models designed for special purposes, which include erosion, strain-rate effects, and crack extension, etc.[82]. The Winfrith Concrete Model[83,84] uses three invariants and four parameters, taking account of strain-rate effects according to the CEB[85] recommendations. This model has been validated for a number of impact and blast cases. Other models in LS-DYNA[86] include Type 16 Pseudo Tensor Concrete/ Geological Model, Type72 Concrete Damage Model, Type 78 Soil/Concrete Model with erosion and Type 96 Brittle Damage Model[87]. The RHT concrete model was developed by Riedel[88], *et al.* and implemented in the general release of AUTODYN[88,89]. Various concrete material models available in the literature are

- Drucker-Prager/cap model
- Winfrith concrete model
- Pseudo tensor concrete/geological model
- Concrete damage model
- Soil/concrete model
- Brittle damage model
- Schwer Murray cap model
- RHT concrete model
- Johnson and Holmquist concrete model (JH model)
- Gebbeken and Ruppert concrete model (GR model)

Despite the extensive research effort, especially in the case of reinforced concrete structures, there is still a need to develop a reliable material model capable of representing the complex behaviour of different types of concrete structures, and therefore it is still an active area of research.

5.5 Observations

Various techniques namely, smeared model, embedded model, and discrete model, are available for FEM of reinforced concrete structural components. The techniques are to be employed depending on the application and degree of accuracy. Many material models are available to represent the complex behaviour of the concrete structures subjected to impact loads. Each material model has its own merits and limitations. Several contact algorithms are available in the literature, namely, frictional sliding, single-surface contact, nodes impacting on a surface, tied interfaces, etc. Appropriate contact algorithm has to be employed for representation of realistic behaviour. From the review, it is observed that the concrete damage model exhibits better performance compared to other material models.

6.   CONCLUSIONS

Extensive literature review has been carried out on concrete structural components subjected to impact loading. Critical review of empirical formulae, analytical models, and numerical simulation techniques have been presented. Empirical formulae on penetration depth, perforation and scabbing limits, as well as their range of applications have been presented. It is observed that the information available on the validation of these models is limited. Hence, there is wider scope to study and validate some of the well known empirical formulae. Penetration resistance functions play an important role in any analytical model. It is observed that the major limitation is rigid projectile assumption. Hence there is scope to develop new/improved analytical models to represent projectile characteristics. The numerical simulation of concrete structural components subjected to impact loads is a complex phenomenon. It is observed that employing appropriate material model for concrete, equation-of-state, contact algorithm and definition of yield surface plays significant role in the accurate simulation of concrete structural components subjected to impact loads. Further, it is observed that current state-of-the-art knowledge available in this area is not adequate for accurate simulation. Hence, there is need and scope to develop new methodologies in terms of development of new/improved material models and contact algorithms, which can be employed in nonlinear explicit finite element analysis of concrete structural components subjected to impact loading.

REFERENCES

1.   Kai, Xu. & Yong, Lu. Numerical simulation study of spallation in reinforced concrete plates subjected to blast loading. *Computers and Structures,* 2006, **84**, 431-38.

2.   Wang, Zhi-liang.; Yong-chi, Li.; Shen, R.F. & Wang, J.G. Numerical study on craters and penetration of concrete slab by ogive-nose steel projectile. *Computers and Geotechnics*, 2007, **34**, 1-9.

3.   Fariborz.; Vossoughi.; Claudia, P.; Ostertag; Paulo, J.M.; Monteiro.; George C. & Johnson. Resistance of concrete protected by fabric to projectile impact. *Cement Concrete Res.*, 2007, **37**, 96-106.

4.   Avraham, N.; David, Z. Dancygier; Yankelevsky & Chanoch Jaegermann. Response of high performance concrete plates to impact of non-deforming projectiles. *Int. J. Impact Eng.*, 2007, **34**, 1768-779.

5.   Beppu, M.; Miwa, K.; Itoh, M.; Katayama, M. & Ohno, T. Damage evaluation of concrete plates by high-velocity impact. *Int. J. Impact Eng.*, 2008, **35**, 1419-426.

6   Song, W.; Ning, J. & Wang, J. Normal impact of truncated oval-nosed projectiles on stiffened plates. *Int. J. Impact Eng.*, 2008, **35**, 1022-034.

7.   Sakdirat; Kaewunruen; Alex, M. & Remennikov. Dynamic flexural influence on a railway concrete sleeper in track system due to a single wheel impact. *Eng. Failure Anal.*, 2009, **16**, 705-12.

8.   Booker, Paul M.; Cargile, James D.; Kistler, Bruce L.; La,Valeria & Saponara. Investigation on the response of segmented concrete targets to projectile impacts. *Int. J. Impact Eng.*, 2009, 1-14.

9.   Hanchak, S.J.; Forrestal, M.J.; E.R. & Youngand Ehrgott. J.Q. Perforation of concrete slabs with 48 MPa (7 ksi) and 140 MPa (20 ksi)unconfined compressive strengths. *Int. J. Impact Eng.*,1992, **12**(1), 1-7.

10.   David, Z. & Yankelevsky. Local response of concrete slabs to low velocity missile impact. *Int. J. Impact Eng.*, 1997, **19**(4), 331-43.

11.   Teland, J.A. & Sjol, H. An examination and reinterpretation of experimental data behind various empirical equations for penetration into concrete. *In* 9th International Symposium Interaction of the Effects of Munitions with Structures, 1999.

12.   Hakan & Hansson, A. Note on empirical formulas for the prediction of concrete penetration. *In* Weapons and Protection, 1942, FOI-Swedish Defence Research Agency, Tumba, SE-147, Vol. 25, Nov. 2003.

13.   Samuely, F.J. & Hamann, C.W. Civil protection. The Architectural Press, 1939.

14.   Amirikian, A. Design of protective structures. Bureau of Yards and Docks, Department of the Navy, 1950. Report No. NT-3726 ,

15.   Kennedy, R.P. A review of procedures for the analysis and design of concrete structures to resist missile impact effects. *Nucl. Eng. Design*, 1976, **37**, 183-203.

16.   Beth, R.A. Penetration of projectiles in concrete. PPAB Interim Report No. 3. 1941.

17.   Gwaltney, R.C. Missile generation and protection in light water-cooled reactor power plants. Oak Ridge National Laboratory, TN. ORNL NSIC-22. 1968.

18.   Chelapati, CV.; Kennedy, RP. & Wall, I.B. Probabilistic

assessment of hazard for nuclear structures. *Nucl. Eng. Design*, 1972, **19**, 33-64.

19. Adeli, H. & Amin, A.M. Local effects of impactors on concrete structures. *Nucl. Eng. Design*, 1985, **88**, 301-17.

20. Linderman, R.B.; Fakhari, M. & Rotz, J.V. Design of structures for missile impact. Rev.1, Bechtel Power Corporation, San Francisco,1973, BC-TOP-9,

21. ACE. Fundamentals of protective structures. Army Corps of Engineers, 1946. Office of the Chief of Engineers, Report No. AT120 AT1207821,

22. NDRC. Effects of impact and explosion. Summary Technical Report Division 2, 1, National Defence Research Committee, Washington, DC, 1946.

23. Kennedy, R.P. Effects of an aircraft crash into a concrete reactor containment building. Holmes & Narver Inc. Anaheim, CA1966.

24. Whiffen, P. U.K. Road Research Laboratory. Note No. MOS/311. 1943.

25. Bulson, P.S. Explosive loading of engineering structures. E & FN Spon, London, 1997.

26. Kar, A.K. Local effects of tornado generated missiles. *ASCE. J. Struct. Div.*, 1978, **104**(ST5), 809-16.

27. Bangash, M.Y.H. Concrete and concrete structures: Numerical modelling and application. Elsevier Applied Science, London, 1989.

28. Berriaud, C.; Sokolovsky, A.; Gueraud, R.; Dulac, J. & Labrot, R. Local behaviour of reinforced concrete walls under missile impact. *Nucl. Eng. Design*, 1978, **45**, 457-69.

29. Barr, P. Guidelines for the design and assessment of concrete structures subjected to impact. UK Atomic Energy Authority Report. Safety and Reliability Directorate, HMSO, London, 1990.

30. Bechtel Power Corporation. Design of structures for missile impact. Topical Report BC-TOP-9-A. 1974.

31. Rotz, J.V. Results of missile impact tests on reinforced concrete panels. *In* 2nd ASCE Specialty Conference on Structural Design of Nuclear Plant Facilities, New Orleans, LA, 1975.

32. Rotz, J.V. Evaluation of tornado missile impact effects on structures. *In* Proceedings of Symposium on Tornadoes, Assessment of Knowledge and Implications for Man. Texas Technical University, 1976.

33. Sliter, G.E. Assessment of empirical concrete impact formulas. *ASCE J. Struct. Div.*, 1980, **106**(ST5), 1023-045.

34. Bangash, M.Y.H. Impact and explosion: Structural analysis and design. CRC Press, Boca Raton, FL, 1993.

35. Jankov, Z.D.; Shanahan J.A. & White M.P. Missile tests of quarter-scale reinforced concrete barriers. *In* Proceedings of Symposium on Tornadoes, Assessment of Knowledge and Implications for Man. Texas Technical University, Lubbock, TX, 1976.

36. Kavyrchine, M. & Astruc, M. Study on the penetration of reinforced concrete slabs by rigid missiles–experimental study-Part II. *Nucl. Eng. Design*, 1977, **41**, 91-102.

37. Goldstein, S.; Berriaud, C. & Labrot R. Study on the perforation of reinforced concrete slabs by rigid missiles— Experimental study-Part I. *Nucl. Eng. Design*, 1977, **41**, 103-20.

38. Chang, W.S. Impact of solid missiles on concrete barriers. *ASCE J. Struct. Div.*, 1981, **107**(ST2), 257-71.

39. Haldar, A. & Hamieh, H. Local effect of solid missiles on concrete structures. *ASCE J. Struct. Div.*, 1984, **110**(5), 948-60.

40. Hughes, G. Hard missile impact on reinforced concrete. *Nucl. Eng. Design*, 1984, **77**, 23-35.

41. Kojima, I. An experimental study on local behaviour of reinforced concrete slabs to missile impact. *Nucl. Eng. Design*, 1991, **130**, 121-32.

42. Tita, Volnei; de Carvalho, Jonas; & Vandepitte, Dirk. Failure analysis of low velocity impact on thin composite laminates: Experimental and numerical approaches. *Composite Structures*, 2008, **83**(4), 413-28.

43. Silva, M.A.G.; Cismasiu, C. & Chiorean, C.G. Numerical simulation of ballistic impact on composite laminates. *Int. J. Impact Eng.,* 2005, **31**(3), 289-306.

44. Krishnamurthy, K.S.; Mahajan, P. & Mittal, R.K. A parametric study of the impact response and damage of laminated cylindrical composite shells. *Comp. Sci. Technol.*, 2001, **61**(12), 1655-669.

45. Reyes, G. Villanueva & Cantwell, W. J. The high velocity impact response of composite and FML-reinforced sandwich structures. *Comp. Sci. Technol.,* 2004, **64**(1), 35-54.

46. Abdullah, M.R. & Cantwell, W.J. The impact resistance of polypropylene-based fibre–metal laminates. *Comp. Sci. Technol.*, 2006, **66**(11-12), 1682-693

47. Li, Q.M.; Reid, S.R.; Wenb, H.M. & Telfordc, A.R. Local impact effects of hard missiles on concrete targets. *Int. J. Impact Eng.*, 2005, **32**, 224-84.

48. Allen, W.A.; Mayfield, E.B. & Morrison, H.L. Dynamics of a projectile penetrating sand. *J. Appl. Phys.*, **28**(3), 370-76.

49. Forrestal, M.J. & Tzou, D.Y. A spherical cavity-expansion penetration model for concrete targets. *Int. J. Solids Struct.*, 1997, **34**(31-32), 4127-146.

50. Forrestal, J.D.J.; Frew, J.P.; Hickesson & Rohwer, T.A. Penetration of concrete targets with deceleration–time measurements. *Int. J. Impact Eng.*, 2003, **28**, 479-97.

51. Wen, H.M. Penetration and perforation of thick FRP laminates. *Comp. Sci. Technol.*, 2001, **61**, 1163-72.

52. Wen, H.M. Predicting the penetration and perforation of targets struck by projectiles at normal incidence. *Mech. Struct. Mach.*, 2002, **30**(4), 543-77.

53. Li, Q.M. & Chen, X.W. Dimensionless formulae for penetration depth of concrete target impacted by a nondeformable projectile. *Int. J. Impact Eng.,* 2003, **28**(1), 93-7116.

54. Forrestal, M.J. & Luk, V.K. Dynamic spherical cavity expansion in a compressible elastic–plastic *solid*. *ASME, J. Appl. Mech.,* 1988, **55**, 275-79.

55. Forrestal, M.J. & Luk, V.K. Penetration into soil targets.

Int. J. Impact Eng., 1992, **12**, 427-44.

56. Forrestal, M.J.; Tzou, D.Y.; Askari, E. & Longcope, D.B. Penetration into ductile metal targets with rigid spherical-nose rods. *Int. J. Impact Eng.,* 1995, **16**, 699-710

57. Forrestal, M.J.; Altman, B.S.; Cargile, J.D. & Hanchak, S.J. An empirical equation for penetration depth of ogive-nose projectiles into concrete *targets. Int. J. Impact Eng.,* 1994, **15**(4), 395-405.

58. Murff, J.D. & Coyle, H.M. Low velocity penetration of kaolin. *ASCE J. Soil Mech. Found. Div.,* 1973, **99**(SM5), 375-89.

59. Riera, J.D. Penetration, scabbing and perforation of concrete structure hit by solid missile. *Nucl. Eng. Design,* 1989, **115**,121-131.

60. Meyers, M.A. Dynamic behaviour of materials. Wiley, New York, 1994.

61. Chen, W.F. Plasticity in reinforced concrete. McGraw Hill, Inc., New York, 1982.

62. Bazant, Z.P.; Pan, J. & Pijaudier, G. Softening in reinforced concrete beams and frames. *ASCE J. Struct. Eng.,* 1987, **113**(12), 2333-347.

63. Kim, J.K. & Lee, T.G. Nonlinearanalysis of reinforced concrete beams with softening. *Computers and Structures,* 1992, **3**, 567-93.

64. Chan, H.C.; Cheung, Y.K. & Huang, Y.P. Nonlinear modeling of reinforced concrete structures. *Computers and Structures,* 1994, **5**, 1099-1107.

65. Foster, S.J.; Budiono, B. & *Gilbert*. R.I. Rotating crack finite element model for reinforced concrete structures. *Computers and Structures,* 1996, **58**, 43-50.

66. Barzegar, F. & Maddipudi, S. Three-dimensional modeling of concrete structures. II: Reinforced concrete. *ASCE J. Struct. Eng.,* 1997, **123**(10), 1347-356.

67. Kwak, H.G. & Kim, D.Y. Nonlinear analysis of RC shear walls considering tension-stiffening effect. *Computers and Structures*, 2001, 499-517.

68. Mosler, J.& Meschke G. Embedded crack vs. smeared crack models: A comparison of elementwise discontinuous crack path approaches with emphasis on mesh bias. *Comp. Meth. Appli. Mech. Eng.,* 2004, **193**(30-32), 3351-375.

69. Sancho, J.M.; Planas, J.; Cendon, Reyes, D.A.E. & Galvez, J.C. An embedded crack model for finite element analysis of concrete fracture. *Eng. Fracture Mech.,* 2007, **74**(1-2), 75-86.

70. Yang, Z.J. & Jianfei, Chen. Finite element modelling of multiple cohesive discrete crack propagation in reinforced concrete beams. *Eng. Fracture Mech.,* 2005, **72**(14), 2280-297.

71. de Borst, R. & Nauta, P. Non-orthogonal cracks in a smeared finite element model. *Engineering Computations,* 1985, **2**, 35-46.

72. Gupta, A.K. & Akbar, H. Cracking in reinforced concrete analysis. *J. Struct. Eng.,* 1983, **10**, 8, 1735-746.

73. Lin, C.S. & Scordelis, A.C. Nonlinear analysis of RC shells of general form. *ASCE J. Struct. Div.,* 1975, **101**, 523-38.

74. Foster, S.J., Budiona B. & Gilbert, R.I. Rotating crack model for reinforced concrete structures. *Computers and Structures,* 1985, **20**, 225-34.

75. Scordelis, A.C.; Ngo, D. & Franklin, H.A. Finite element study of reinforced concrete beams with diagonal tension cracks. *In* Proceedings of Symposium on Shear in Reinforced Concrete, 1974, ACI Publication SP-42.

76. Th, Y.J. Li & Zimmerman. Numerical evaluation of rotating crack model. *J. Comp. Struct.*, 1998, **69**, 487-97.

77. Yamagushi, E. & Ohta, T. Accurate and efficient method for analysis of reinforced concrete structures. *ASCE J. Struct. Eng.*, 1993, **119**(7), 2017-035.

78. Duan, S.H. & Ye, T.Q. Three-dimensional frictional dynamic contact analysis for predicting low-velocity impact damage in composite laminates. *Adv. Eng. Software,* 2002, **33**(1), 9-15

79. Heinstein, Martin W.; Mello, Frank J.; Attaway, Stephen W. & Laursen, Tod A. Contact—impact modeling in explicit transient dynamics. *Comp. Meth. Appli. Mech. Eng.,* 2000, **187**(3-4), 621-40.

80. Mohammadi, S.; Forouzan-sepehr, S. & Asadollahi, A. Contact based delamination and fracture analysis of composites. *Thin-Walled Structures*, 2002, **40**(7-8), 595-609.

81. Ladeveze, P.; Lemoussu, H. & Boucard, P.A. A modular approach to 3-D impact computation with frictional contact. *Computers and Structures*, 2000, **78**(1-3), 45-51.

82. Agardh, L. & Laine, L. 3D FE-simulation of high-velocity fragment perforation of reinforced concrete slabs. *Int. J. Impact Eng.,* 1999, **22**, 911-22.

83. Ottosen, N.S. Failure criterion for concrete. *ASCE J. Eng. Mech. Div.,* 1975, **103**(EM4), 527-35.

84. Broadhouse, B.J. The Winfrith concrete model in LS-DYNA3D. Atomic Energy Agency, AEA Technology, SPD/ D(95)363, Dorchester, UK, 1995.

85. CEB. CEB-FIP model code 1990. Committee Euro-International Du Beton, Redwood Books, Trowbridge, Wiltshire, UK, 1993.

86. LS-DYNA. Keyword user's manual. Version 950. Non linear dynamic analysis of structures in three dimensions. Livermore Software Technology Corporation (LSTC), Livermore, 1999.

87. Govindjee, S.; Gregory, J.K. & Simo, J.C. Anisotropic modelling and numerical simulation of brittle damage in concrete. *Int. J. Numer. Meth. Eng.*, 1995, **38**(21), 3611-633.

88. Riedel, W. Beton unter dynamishen lasten, meso- und makromechanische modelle und ihre parameter. Ernst Doctoral Thesis. Mach Institute, Freiburg, 2000.

89. Hansson, H. & Agardh, L. Experimental and numerical studies of projectile perforation in concrete tar. *In* Structural failure and plasticity (IMPLAST-2000), *edited by* X.L. Zhao & R.H. Gizebiets. Elsevier Science, Amsterdam, 2000.

Table 1. Various empirical formulae for penetration depth

Imperial units	SI units

(i) *Modified Petry formula*[13-15]

$$x = 12K_p\ A_p \log_{10}\left(1 + \frac{v^2}{215000}\right)$$

$$\frac{x}{d} = K\frac{M}{d^3}\log_{10}\left(1 + \frac{v^2}{19974}\right)$$

K_P = concrete permeability
   = 0.00799 - massive PC,   0.00426 - normal RC
   = 0.00284 - special RC

K = 6.36x10-4 - massive PC,   3.39x10-4 - normal RC
   = 2.26x10-4 - special RC

Remarks: The Petry penetration formula was originally developed in 1910. The modified Petry formula is one of the most common formulae used to predict the penetration depth in an infinite concrete target.

(ii) *Ballistic Research Laboratory, (BRL) formula*[15-19]

$$\frac{x}{d} = \frac{427}{\sqrt{f_c}}\left(\frac{M}{d^3}\right)d^{0.2}\left(\frac{v}{1000}\right)^{1.33}$$

$$\frac{x}{d} = \frac{1.33\text{x}10^{-3}}{\sqrt{f_c}}\left(\frac{M}{d^3}\right)d^{0.2}v^{1.33}$$

Perforation limit is given by, $\dfrac{e}{d} = 1.3\dfrac{x}{d}$

Modified BRL formula for scabbing is[20] $\dfrac{h_s}{d} = 2\dfrac{x}{d}$,

Remarks: The BRL formula was developed to calculate the penetration depth in concrete hit by a rigid projectile.

(iii) *Army Corps of Engineers (ACE) formula*[15, 18, 21]

$$\frac{x}{d} = \frac{282.6}{\sqrt{f_c}}\left(\frac{M}{d^3}\right)d^{0.215}\left(\frac{v}{1000}\right)^{1.5} + 0.5$$

Perforation and scabbing limits are given by

$$\frac{e}{d} = 1.32 + 1.24\frac{x}{d} \text{ for } 1.35 < \frac{x}{d} < 1.35 \text{ or } 3 < \frac{e}{d} < 18$$

$$\frac{h_s}{d} = 2.12 + 1.36\left(\frac{x}{d}\right) \text{ for } 0.65 < \frac{x}{d} \le 11.75 \text{ or } 3 < \frac{h_s}{d} \le 18$$

$$\frac{x}{d} = \frac{3.5\text{x}10^{-4}}{\sqrt{f_c}}\left(\frac{M}{d^3}\right)d^{0.215\ 1.5}v^{1.5} + 0.5$$

Remarks: The proposed expressions for penetration depth are more suitable under missile impacts.

(iv) *Modified NDRC formula*[15, 22, 23]

$$G = \frac{180 NM}{d\sqrt{f_C}}\left(\frac{v}{1000d}\right)^{1.8}$$

$$\frac{x}{d} = 2G^{0.5} \text{ for } G \ge 1$$

G is a function of x/d,

$$G = \left(\frac{x}{2d}\right)^2 \text{ for } \left(\frac{x}{d}\right) \le 2 \quad \text{and}$$

$$G = \frac{x}{d}\ 1\ \text{for } \frac{x}{d} > 2$$

where, N^* = 0.72, 0.84, 1.0 and 1.14 for flat, hemispherical, blunt and very sharp noses respectively.

$$G = 3.8\text{x}10^5\frac{NM}{d\sqrt{f_c}}\left(\frac{v}{d}\right)^{1.8}$$

$$\frac{x}{d} = G + 1 \text{ for } G < 1$$

Perforation limit

$$\frac{e}{d} = 3.19\left(\frac{x}{d}\right) - 0.718\left(\frac{x}{d}\right)^2 \text{ for } \frac{x}{d} \le 1.35 \text{ or } \frac{e}{d} \le 3$$

$$\frac{e}{d} = 1.32 + 1.24\frac{x}{d} \text{ for } < \frac{X}{d} < 1.35 \text{ or } 3 < \frac{e}{d} < 18$$

scabbing limit

$$\frac{h_s}{d} = 7.91\left(\frac{x}{d}\right) 5.06\left(\frac{x}{d}\right)^2 \text{ for } \frac{x}{d} \le 0.65 \text{ or } \frac{h_s}{d} \le 3,$$

$$\frac{h_s}{d} = 2.12 + 1.36\left(\frac{x}{d}\right) \text{ for } 0.65 < \frac{x}{d} \le 11.75 \text{ or } 3 < \frac{h_s}{d} \le 18$$

Remarks: This formula was proposed in 1946 by the US National Defense Research Committee based on ACE formulae. It was assumed that the contact force increased linearly to a constant maximum value when the penetration depth is small.

(v) *Whiffen formula*[24, 25]

$$\frac{x}{d} = \left(\frac{870}{f_c^{0.5}}\right)\left(\frac{M}{d^3}\right)\left(\frac{d}{a}\right)^{0.1}\left(\frac{V_0}{1750}\right)^n \text{ with } n = \frac{10.70}{f_C^{0.25}}$$

$$\frac{x}{d} = \left(\frac{2.61}{f_c^{0.5}}\right)\left(\frac{M}{d^3}\right)\left(\frac{d}{a}\right)^{0.1}\left(\frac{v_0}{533.4}\right)^n, \text{ with } n = \frac{97.51}{f_c^{0.25}}$$

Where, a = maximum aggregate size
Valid ranges:
800<f_c<10,000(psi)0.3<M<22,000(lb)   0.5<d<38(in)
0<V_0<1750(ft/s) and 0.5<d/a<50 for ogival projectile nose shapes of caliber radius between 0.8 and 3.5.

Ranges   of   application: 5.52<f_c<68.95(MPa)
0.136<M<9979.2(kg)   12.7<d<965.2(mm)
0<V_0<1127.8(m/s).

Remarks: This formula was proposed based on the extensive range of wartime data from penetration studies of fragments on reinforced concrete and investigations involving larger ranges of projectile diameter and concrete aggregate size.

Table 1. Contd..

Imperial units	SI units

(vi) *Amman and Whieney formula Kennedy*[15]

$$\frac{x}{d} = \frac{282NWd^{0.2}}{d^3 f_c^{0.5}}\left(\frac{v}{1000}\right)^{1.8}$$

$$\frac{x}{d} = \frac{6 \times 10^{-4}}{f_c^{0.5}} N(M/d^3)d^{0.2}v^{1.8}$$

Remarks: This formula was proposed to predict the penetration of explosively generated small fragments at relatively high velocities (>300 m/s). This formula is in similar form to the ACE formula and the NDRC formula. N* is the nose shape defined in the NDRC formula.

(vii) *Kar formula* [26, 27]

$$G = \frac{180N^*M}{d\sqrt{f_c}}\left(\frac{E}{E_s}\right)^{1.25}\left(\frac{V_0}{1000d}\right)^{1.8} \text{ where,}$$

$$G = 3.8 \times 10^{-5}\left(\frac{E}{E_s}\right)^{1.25}\frac{N^*M}{d\sqrt{f_c}}\left(\frac{V_0}{d}\right)^{1.8}$$

$$\frac{x}{d} = 2G^{0.5} \text{ for } G \geq 1 \text{ and } \frac{x}{d} = G+1 \text{ for } G < 1$$

The scabbing limit is given by

Where, E and E_s are the Young's moduli of the projectile and steel respectively.

The perforation limit is given by

$$\frac{e-a}{d} = 3.19\left(\frac{x}{d}\right) - 0.718\left(\frac{x}{d}\right)^2 \text{ for } \frac{x}{d} \leq 1.35$$

$$\frac{e-a}{d} = 1.32 + 1.24\left(\frac{x}{d}\right) \text{ for } 1.35 < \frac{x}{d} \leq 13.5$$

$$\frac{h_s-a}{d}b = 7.19\left(\frac{x}{d}\right) - 5.06\left(\frac{x}{d}\right)^2 \quad \text{for } \frac{x}{d} £ \, 0 \, 65$$

$$\frac{h_s-a}{d}b = 2.12 + 1.36\left(\frac{x}{d}\right) \quad 0\,65 < \frac{x}{d} < 11\,75$$

where, $b = (E_s/E)^{0.2}$.

Remarks: NDRC formula was modified to obtain this empirical formula using regression analysis to account for both the size of aggregate and the type of missile material in terms of Young's modulus *E*. If the material of the projectile is steel, the penetration depth prediction formula is identical to the modified NDRC formula.

(viii) *CEA–EDF perforation formula* [28]

Not available

Perforation limit formula,

$$\frac{e}{d} = 0.82\frac{M^{0.5}V_0^{0.75}}{\rho_c^{0.125}f_c^{0.375}d^{1\,5}}, \; \rho_c = \text{density of concrete.}$$

The ballistic limit V_p(m/s), $V_p = 1.3\rho_c^{1/6}f_c^{0.5}\left(\frac{dH_0^2}{M}\right)^{2/3}$

where, H_0 is the thickness of the target

Remarks: Based on a series of drop-weight and air gun tests, CEA and EDF predicted ballistic performance of reinforced concrete slabs under missile impact.

(xi) *UKAEA formula*[29]

$$G = \frac{180NM}{d\sqrt{f_c}}\left(\frac{v}{1000d}\right)^{1.8}$$

$$G = 3.8 \times 10^{-5}\frac{NM}{d\sqrt{f_c}}\left(\frac{v}{d}\right)^{1.8}$$

$$\frac{x}{d} = 0.275 - [0.0756 - G]^{0.5} \text{ for } G \leq 0.0726, \; \frac{x}{d} = [4G - 0.242]^{0.5} \text{ for } 0.0726 \leq G \leq 1.0605 \; \frac{x}{d} = G + 0.9395 \text{ for } G \geq 1.0605$$

Remarks: Based on extensive studies of the protection of nuclear power plant structures in UK, Barr incorporated further modification to NDRC formula, to account for the impact velocities.

(x) *Bechtel formula* [30-34]

$$\frac{h_s}{d} = \frac{15.5M^{0.4}V_0^{0.5}}{f_c^{0.5}d^{1.2}}$$

The Bechtel formula for the scabbing limit for steel pipe missiles is

$$\frac{h_s}{d} = \frac{5.42M^{0.4}V_0^{0.65}}{f_c^{0.5}d^{1.2}}$$

$$\frac{h_s}{d} = 38.98\left(\frac{M^{0.4}V_0^{0.5}}{f_c^{0.5}d^{1.2}}\right)$$

$$\frac{h_s}{d} = 13.63\left(\frac{M^{0.4}V_0^{0.65}}{f_c^{0.5}d^{1.2}}\right)$$

Remarks: This formula for the scabbing limit was developed by Bechtel Power Corporation and is based on test data applicable to missile impacts on nuclear-plant structures. The formula is essentially restricted to hard projectiles such as a solid steel slug or rod.

Table 1. Contd..

Imperial units	SI units

(xi) *Stone and Webster formula*[33, 35]

$$\frac{h_S}{d} = \left(\frac{MV_0^2}{Cd^3}\right)^{1/3}$$ in which the dimensional coefficient *C* is dependent on the ratio of the target thickness (H_0) to the projectile

diameter *(d)*. For solid projectiles, *C* in Imperial units varies between 900 and 950 for H_0/d between 1.5 and 3.0.
If SI units are used, C varies from 0.35 to 0.37 when H_0/d varies from 1.5 to 3.0. A linear relationship may be employed for calculation of *C*, i.e. $C = 33.3(H_0/d) + 850.0$ in imperial units or $C = 0.013(H_0/d) + 0.330$ in SI units. The range of test parameters for this formula is $20.7(\text{MPa}) \leq f_c \leq 31.0(\text{MPa})$ and $1.5 \leq h_s/d \leq 3.0$.
Remarks: This formula agrees very well with most of the experimental results.

(xii) *Degen perforation formula*[28, 36, 37]

Not available

$$\frac{e}{d} = 0.69 + 1.29\left(\frac{x}{d}\right) \quad \text{for } 2.65 \leq \frac{e}{d} \leq 18 \quad \text{or } 1.52 \leq \frac{x}{d} \leq 13.42$$

$$\frac{e}{d} = 2.2\left(\frac{x}{d}\right) - 0.3\left(\frac{x}{d}\right)^2 \quad \text{for } \frac{e}{d} < 2.65 \text{ or } \frac{x}{d} < 1.52$$

where x is determined from the modified NDRC formula.
valid ranges: $28.4 < f_c < 43.1(\text{MPa})$, $25.0V_0 \leq 311.8(\text{m/s})$, $0.15 < H_0 < 0.61(\text{m})$ and $0.10 < d < 0.31(\text{m})$.

Remarks: Based on a statistical analysis of the experimental data.

(xiii) *Chang formula*[38]

Not available

Considering a flat ended steel cylinder impacting a reinforced concrete panel, Chang suggested a perforation limit,

$$\frac{e}{d} = \left(\frac{u}{V_0}\right)^{0.25}\left(\frac{MV_0^2}{d^3 f_c}\right)^{0.5} \quad \text{and} \quad \frac{h_s}{d} = 1.84\left(\frac{u}{V_0}\right)^{0.13}\left(\frac{MV_0^2}{d^3 f_c}\right)^{0.4} \quad \text{where}$$

u is a reference valid range: velocity
$16.0 \leq v_0 \leq 311.8(\text{m/s})$, $0.11 \leq M \leq 342.9(\text{kg})$,
$50.8 \leq d \leq 304.8(\text{mm})$ and $22.8 \leq f_c \leq 45.5(\text{MPa})$.

Remarks: First of its kind to use dimensionally homogenous equations.

(xvi) *Haldar–Hamieh formula*[39]

Not available

$$\frac{x}{d} = 0.0308 + 0.25251 I_a, \quad 0.3 \leq I \leq 4, \quad \frac{x}{d} = 0.6740 + 0.567 I_a, \quad 4 < I \leq 21,$$

$$\frac{x}{d} = 1.1875 + 0.0299 I_a, \quad 21 < I \leq 455 \quad I_a = \frac{WNv^2}{gd^3 f_c}$$

(xv) *Adeli & Amin formula*[19]
Penetration, perforation and scabbing are given by

$$\frac{x}{d} = 0.0416 + 0.1698 I_a - 0.0045 I_a^2 \quad \text{for } 0.3 < I_a < 4 \quad \frac{x}{d} = 0.0123 + 0.169 I_a - 0.0081 I_a^2 + 0.0001 I_a^3 \quad \text{for } 4 \leq I_a < 21$$

$$\frac{e}{d} = 1.8685 + 0.4035 I_a - 0.0114 I_a^2 \quad \text{for } 0.3 < I_a < 21 \text{ and } \frac{h_s}{d} = 0.9060 + 0.3214 I_a - 0.0106 I_a^2 \quad \text{for } 0.3 < I_a < 21$$

which are subject to the restrictions, i.e $27 < V_o < 312(\text{m/s})$, $0.7 < H_o/d < 18$, $0.11 < M < 343(\text{kg})$, $d \leq 0.3(\text{m})$ and $x/d \leq 2.0$
Remarks: Based on the impact factor I_a defined by[38]

(xvi) *Healey and Weissman formula*[27]

$$G = \frac{206.5N * M}{d\sqrt{f_c}}\left(\frac{E}{E_s}\right)\left(\frac{V_o}{1000d}\right)^{1.8}, \text{where}$$

$$\frac{x}{d} = 2G^{0.5} \quad \text{for } G \geq \text{ and } \frac{x}{d} = G+1 \quad \text{for } G < 1$$

$$G = 4.36 \times 10^{-5}\left(\frac{E}{E_s}\right)\frac{N * M}{d\sqrt{f_c}}\left(\frac{V_o}{d}\right)^{1.8}$$

Remarks: Similar to the modified NDRC formula and the Kar formula

Table 1. Contd..

Imperial units	SI units

(xvii) *Hughes*[40]

$$\frac{x}{d} = 0.19 \frac{N_h I_h}{S},$$

where N_h is a projectile nose shape coefficient, which is 1.0, 1.12, 1.26 and 1.39 for flat, blunt, spherical and very sharp noses, respectively. I_h is a non-dimensional impact factor defined by

$$I_h = \frac{M V_0^2}{d^3 f_t} \quad \text{and} \quad S = 1.0 + 12.3 \ \text{In}(1.0 + 0.03 I_h)$$

The perforation and scabbing limits are predicted by

$$\frac{e}{d} = 3.6 \frac{x}{d} \quad \text{for } \frac{x}{d} < 0.7 \quad \frac{e}{d} = 1.58 \frac{x}{d} + 1.4 \quad \text{for } \frac{x}{d} \geq 0.7, \quad \frac{h_s}{d} = 5.0 \frac{x}{d} \quad \text{for } \frac{x}{d} < 0.7 \quad \frac{h_s}{d} = 1.74 \frac{x}{d} \ 2.3 \quad \text{for } \frac{x}{d} \geq 0.7,$$

The formulae were verified in the range of available test data for $I_h < 3500$. However, they are conservative when $I_h < 40$ and $H_o/d < 3.5$.

Remarks: Based on assumption that the penetration resistance increases linearly in the initial stages and then decreases parabolically with the penetration depth.

(xviii) *IRS formula*[34]

Not available

$$x = 3703.376 f_c^{-0.5} + 82.152 f_c^{-0.18} \ \exp[-0.104 f_c^{0.18}]$$

Formula for total protection of a target against penetration, perforation and scabbing is

$$\text{SVOLL} = 3913.119 f_c^{-0.5} + 132.409 f_c^{-0.18} \ \exp(-0.104 f_c^{0.18})$$

Remarks: Requires only compressive strength of concrete

(xix) *Criepi formula*[41]

Not available

$$\frac{x}{d} = \frac{0.0265 N^* M d^{0.2} V_0^2 (114 - 6.83 \ \text{x} \ 10^4 f_c^{2/3})}{f_c^{2/3}} \left[\frac{(d + 1.25 H_r) \ H_r}{(d + 1.25 H_o) \ H_o} \right]$$

in which $H_r = 0.2$m is the reference thickness of the slab.

$$\frac{e}{d} = 0.90 \left(\frac{u}{V_o} \right)^{0.25} \left(\frac{M V_0^2}{d^3 f_c} \right)^{0.5} \quad \text{and} \quad \frac{h_s}{d} = 1.75 \left(\frac{u}{V_o} \right)^{0.13} \left(\frac{M V_0^2}{d^3 f_c} \right)^{0.4},$$

where, $u = 61$ m/s is the reference velocity

Remarks: Modified form of Chang's[37] formula

The perforation and scabbing limits which are determined by non-dimensional numbers and therefore independent of a particular unit system.

(xx) *Conwep formula*[12]

$$x = \frac{222 \ N \ W \ v^{1.8}}{d^{1.8} \ f_c^{0.5}} + d \quad \text{for } x > 2d$$

N = Nose shape factor or nose performance coefficient
$\quad = 0.72 + 0.25 \ (CRH - 0.25)^{0.5}$
where, CRH = caliber radius head, i.e. ratio between ogive radius and the projectile diameter

$$x = \frac{11.76 \ N \ M \ v^{1.8}}{d^{1.8} \ f_c^{0.5}} + d, \text{for } x > 2d$$

Remarks: Widely used formula and generally agrees well with experimental values.

Note:
M	Mass of the projectile, lb (Imperial) or kg (SI)
f_c	Unconfined compressive strength of concrete, psi (imperial) or MPa (SI)
d	Diameter of the projectile, inch (imperial) or m (SI)
x	Penetration depth, ft (imperial) or m (SI)
v	Impact velocity, ft/s (imperial) or m/s (SI)
h_s	Scabbing limit, inch (imperial) or m (SI)

Contributor

Mr A. Rama Chandra Murthy is working as Scientist in Structural Engineering Research Centre, Council of Scientific and Industrial Research. He has published more than 45 papers including international journals, national journals, and conference proceedings. His research areas include: fracture analysis, impact analysis, finite element analysis, and masonry structures.